"Power Holes" and Nonlinear Forward and Backward Wave Gain Competition in Helix Traveling-Wave Tubes

David Chernin, Thomas M. Antonsen, Jr., *Member, IEEE,* and Baruch Levush, *Fellow, IEEE*

***Abstract*—The output power of a forward wave linear beam amplifier like a helix traveling-wave tube (TWT) can show unexpected dips as a function of drive signal frequency in certain narrow frequency ranges. These dips, commonly called "power holes," can have serious consequences for the performance of the system of which the amplifier is a part. It is widely believed that these power holes, which only occur under large signal conditions, are due to the amplification of a backward wave space harmonic of a signal at a harmonic of the drive signal frequency, when the frequency of that harmonic happens to fall in the range of frequencies in which backward wave gain occurs. The resulting growth of the backward wave can compete with the forward wave gain, resulting in a reduction of output power at the drive frequency. Power holes can occur under conditions for which the backward wave oscillator (BWO) instability does *not* occur, i.e., the backward wave gain is finite, not infinite. In this paper, we report on a study of power holes using the large signal helix TWT code, CHRISTINE 3D. In particular we demonstrate the connection between backward wave gain and the depth of the power holes. We show that the frequency range over which backward wave gain occurs can be different than that predicted by small signal BWO theory when a large amplitude forward wave signal is present. This effect is due to the destabilization of the *fast* beam space charge wave, interacting with the backward wave under large signal conditions. We review commonly used methods to reduce the backward wave gain, and argue that any of these should reduce the depth of the power holes. The choice of one or another gain reduction method will depend on various engineering design constraints, and on cost. We suggest that a code like CHRISTINE 3D can be helpful in making this choice.**

***Index Terms*—Backward wave oscillators (BWO), microwave amplifiers, simulation, stability, traveling-wave tube (TWT).**

I. Introduction

THE GENERATION and amplification of backward waves in forward-wave traveling-wave amplifiers are fundamental processes that can severely limit the attainable performance of these devices [1]–[3]. As a consequence, designers are frequently faced with performance optimization problems that are constrained by the strength of the interaction between the electron beam and the backward waves supported by the slow wave circuit. For example, when attempting to increase the forward wave gain by increasing beam current or interaction length, a threshold will eventually be reached at which the gain of the backward wave becomes infinite, leading to spontaneous backward wave oscillation (BWO) [4]–[7]. A substantial body of both theoretical and practical engineering knowledge has been developed over the years on techniques for the suppression of BWO [2],[8], including the introduction of attenuation, severed or tapered [9],[10] circuits, and (more recently) tapered magnetic fields [11]. Even below the BWO threshold, however, the finite gain of the backward wave can compete under certain conditions with the gain of the fundamental amplifying wave, leading to dips in the output power versus frequency curves; such dips can occur when a harmonic of the drive signal falls in a frequency band in which the backward wave gain is finite, leading to gain of a wave reflected from a discontinuity, as it propagates back toward the input. Though no oscillation is necessarily involved, it is common to refer to these dips as "BWO power holes." If large enough, these power holes can have serious consequences for the performance of the systems in which the amplifier is employed.

BWO power holes have not been extensively discussed in the published literature to our knowledge[1], though they are of course well known and have been widely observed by traveling-wave tube (TWT) manufacturers and their customers. In fact, we are aware of only one other published paper on the subject, by Dionne, Harper, and Krahn [12]. These authors present and discuss results from a novel disk model large signal code in which the disks are divided into angular sectors, in order to resolve the angular dependence of the backward wave. They successfully simulate a power hole using their code. The disks in this model maintain a fixed radius as they propagate through the interaction space. This treatment may not be fully consistent, therefore, under large signal conditions in which significant beam expansion occurs. Since the strength of the interaction between the beam and the backward wave is sensitive to beam radius, this effect is important to include, that is, a fully consistent model of power holes should be three-dimensional, permitting electron motion, and electromagnetic field variations, in radius, azimuth, and axial location.

The present paper illustrates the phenomenon of power holes using CHRISTINE 3D [13], a three–dimensional (3-D) large

Manuscript received August 22, 2003. This work was supported by the Office of Naval Research.The review of this paper was arranged by Editor D. Goebel.

D. Chernin is with Science Applications International Corporation, McLean, VA 22102 USA (e-mail: chernind@saic.com).

T. M. Antonsen, Jr. is with the Institute for Research in Electronics and Applied Physics, University of Maryland, College Park, MD 20742 USA.

B. Levush is with the Naval Research Laboratory, Washington, DC 20875 USA.

Digital Object Identifier 10.1109/TED.2003.819252

[1]An unpublished report by D.P Hinson entitled, "An investigation of power suck-out in helix traveling-wave tubes," [Varian Associates AFOSR-TR-79-0392 (Dec. 1978)] was brought to our attention by an anonymous referee. It is available at www.ntis.gov, document ADA067916.

signal, steady-state simulation code for helix TWTs. CHRISTINE 3D includes the self-consistent effects of beam expansion, as described above. The code divides the beam into rays, permitting resolution in radius, angle, and rf phase. Circuit fields and space charge fields for the backward wave vary in all three dimensions; for the forward wave the fields are independent of azimuth, but vary radially and axially. CHRISTINE 3D has been used successfully to simulate the performance of TWTs in several different frequency bands. After illustrating the physical mechanisms responsible for the appearance of power holes, the code is used below to simulate a power hole under large signal conditions, and to illustrate various strategies for reducing the depth of power holes.

This paper is organized as follows. Section II following this introduction describes in some detail the physical mechanisms, including harmonic generation, reflection, and backward wave gain, which combine to produce a power hole. Results from CHRISTINE 3D are used to illustrate these mechanisms individually and in combination to produce a power hole. Techniques for the reduction of the depth of a power hole are reviewed in Section III. One of these, a recently proposed, novel strategy to control backward wave gain by tapering the magnetic field, is studied in some detail for its effect on the power holes using CHRISTINE 3D. A summary and some conclusions are given in Section IV.

II. Physics of Power Holes

BWO power holes in forward-wave linear beam amplifiers are fundamentally caused by a competition between the amplification of the forward-going injected signal and amplification of a backward-going (reflected) signal at a harmonic of the injected signal. The basic synchronism conditions between the beam and the forward and backward waves required for this competitive amplification are illustrated in the dispersion diagram of Fig. 1. In a perfect, lossless forward wave structure[2] with perfectly matched ends, only the injected signal and its harmonics[3] with positive group velocities will be present, curves of which are represented as solid lines in Fig. 1. The beam will interact strongly with the wave in a range of frequencies—labeled "operating band" in Fig. 1—such that the slow-beam space charge wave is nearly synchronous with the fundamental space harmonic of the circuit. This is the familiar amplification process responsible for signal amplification in all forward wave TWTs.

When one of the harmonics of a signal in the operating band (Fig. 1) is reflected from a circuit discontinuity, the first spatial harmonic of the reflected wave ($v_g < 0$) can also be in synchronism with the slow beam mode, as shown in the figure.

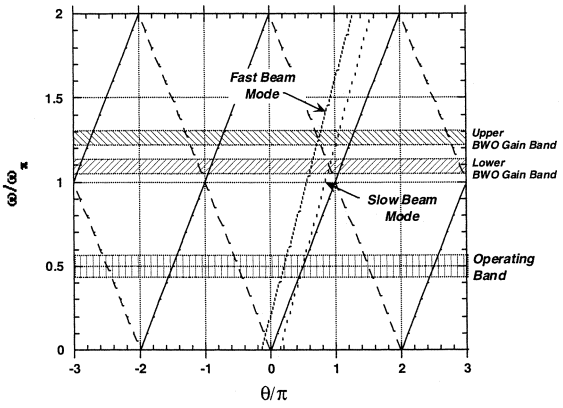

Fig. 1. Dispersion diagram for a simple forward wave structure. Frequency is normalized to the π-mode frequency and phase shift per pitch, θ, is normalized to π. The dispersion relations for the fast (+) and slow (-) beam modes, $\omega - k_z v_{beam} = \pm\bar{\omega}_p$, where $\bar{\omega}_p$ is the effective plasma frequency, are also shown. Solid lines indicate spatial harmonics of a wave having positive group velocity (power flow from input to output end of tube); dashed lines indicate negative group velocity (reflected waves). The operating band is determined in part by the degree of synchronism between the beam and the fundamental spatial harmonic of the forward wave; the BWO gain bands are similarly determined by the degree of synchronism between the beam modes and the first spatial harmonic of the reflected wave. Under small signal conditions, the backward wave gain is positive in the lower BWO gain band and negative in the upper BWO gain band.

Under small signal conditions, the unstable interaction of the slow beam mode and the circuit mode leads to positive gain of the reflected wave in a band of frequencies labeled "lower BWO gain band" in Fig. 1.

It is interesting and, as it turns out, important to note that the first spatial harmonic of the reflected wave can also be in synchronism with the fast beam mode, as shown in the figure and labeled "upper BWO gain band". Under small signal conditions, signals in this range of frequencies are attenuated, that is, the small signal backward wave gain is negative, as the beam absorbs energy from the wave.

Now, if the first spatial harmonic of the reflected signal experiences positive gain, then this process will take energy from the beam and so will compete with the desired amplification of the injected signal(s). This gain competition is the basic process responsible for power holes. Harmonic generation, reflection, and backward wave gain must be all present. Note that no band gap near the pi-point is necessary for this phenomenon to occur, though the presence of such a gap and its associated zero group velocity will increase the backward wave gain by increasing the coupling between the forward and reflected waves [14].

The interesting thing that we have found is that as the drive power of the main signal is increased, the small signal backward wave gain decreases in the lower BWO gain band of Fig. 1, while it increases and eventually changes sign as the drive power is increased, in the upper BWO gain band. The result is that, in our example, a power hole occurs in the upper band, and not in the lower band, as one would expect from small signal analysis. A detailed analysis of this effect is underway and results will be published in a future paper.

In order to demonstrate this and other relevant effects using CHRISTINE 3D, we consider a helix TWT with basic parameters listed in Table I. The tube is basically a modified C-band design, which has been used many times for the validation of

[2]A slow wave circuit is by convention designated as a "forward wave circuit" if the phase and group velocities of the lowest mode have the same sign in the fundamental Brillouin zone, $-\pi < \theta < \pi$, as in Fig. 1. A helix is an example of a forward wave circuit. A reflected wave on a forward wave circuit is still a forward wave, by this definition. Spatial harmonics of a wave on a forward-wave circuit can have phase and group velocities with different signs. These backward-wave spatial harmonics are sometimes, a little confusingly, called backward waves.

[3]If multiple signals at different frequencies are present, intermods will be generated. These only complicate the analysis and do not change the fundamental features of the interactions between the beam and the circuit waves described in this paper. We therefore confine ourselves to the case of a single frequency input signal.

TABLE I
BASE CASE PARAMETERS FOR CHRISTINE 3D SIMULATIONS

Quantity	Value
Beam current	0.170 A
Beam voltage	2.5 kV
Beam radius	0.060 cm
Helix pitch	0.080 cm
Helix radius	0.124 cm
Magnetic field	-1400 G
Interaction length	9.58 cm

the CHRISTINE and CHRISTINE 3D codes, except that it is simulated in a parameter range for which it was not designed, but which nominally satisfies our requirements that the backward wave second harmonic experiences gain in the range of frequencies (8–9 GHz) at which we are driving it. A tape helix model [15] is used to compute the phase velocities and interaction impedances of both forward and backward waves. The circuit is narrow band; no vanes are included. There is no linear forward wave gain at the second harmonic[4]. For the study reported here, no sever is present and the circuit is taken to be completely lossless in order to maximize the effects that we are studying.

The beam is initialized as a "rigid rotor", of a specified radius in the 1400 G solenoid focusing field. This means that the individual simulation particles are assigned an initial value of azimuthal velocity such that the radial forces (centrifugal, centripetal, and space charge electric field) are in balance. This is a slight generalization of Brillouin flow, in which the radial forces are also in balance, but the additional assumption is made that all particles are launched from a field free cathode, which leads to a constraint among the beam voltage, beam current, beam radius, and magnetic field. The negative value of magnetic field means that the direction of the field is from the output end toward the input end of the tube.

CHRISTINE 3D is used to compute small signal backward wave gain for this tube, as follows: A number of very small amplitude backward waves, with frequencies spaced equally between 16.5 and 18.0 GHz are introduced. The initial amplitudes, at the input end of the tube, are chosen to be sufficiently small that the backward waves remain in the linear regime and no interference occurs among them. The wave amplitudes are integrated along the interaction space, according to the prescription in [14], from input to output. The backward wave gain (in dB) for each wave is defined to be

$$g_{BW} \equiv 20 * \log_{10}\left(\frac{A(z_1)}{A(z_2)}\right) \tag{1}$$

where $A(z)$ is the backward wave amplitude as a function of z, and where z_1 and z_2 are defined as follows: If $\partial A(z)/\partial z \geq 0$ for all $0 \leq z \leq L$, where L is the interaction length, then $z_1 = 0$, $z_2 = L$, and the backward wave gain is negative. If, however, $\partial A(z)/\partial z < 0$ for at least one interval in z, then

[4]We have tested this assertion by running CHRISTINE 3D with low-level drive signals in the range of 16–18 GHz.

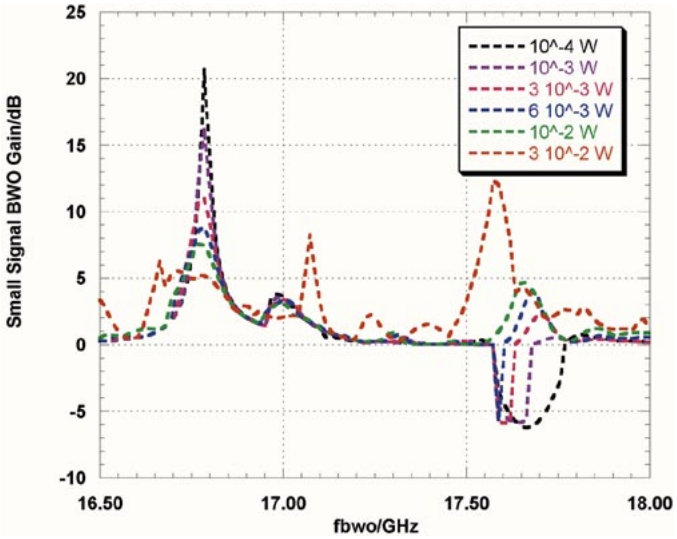

Fig. 2. Small signal backward wave gain as a function of frequency, for various values of drive power. The drive frequency is 8.40 GHz.

$A(z_1)$ is the maximum amplitude and $A(z_2)$ is the minimum amplitude, for $z_2 > z_1$.

When backward wave gain is plotted versus frequency for the tube with parameters in Table I, we obtain the dependence shown in Fig. 2. We see that when the drive power is small (10^{-4} W, or $-$ 10 dBm), the small signal backward wave gain is positive in a small frequency range centered at approximately 16.75 GHz, and it is negative in a small frequency range centered at approximately 17.70 GHz. We interpret this result as the expected small signal phenomena of unstable interaction of the slow beam mode with the backward wave in the lower band, and damped interaction of the fast beam mode with the backward wave in the upper band[5].

As the drive power is increased, however, we see in Fig. 2 that the gain in the lower band decreases and the gain in the upper band increases until, for some level of drive power, the gain in the upper band becomes positive[6]. The bunching of the beam by the large drive signal may be responsible for this effect, though the exact mechanism remains to be clarified. We find that this effect is not sensitive to the drive frequency. An observed slight downward shift of the frequency for peak BWO gain may be understood as the effect of the slowing down of the beam under large signal conditions. As the drive power is further increased, the gain in the upper band can exceed the gain in the lower. A consequence is that, at least for the present example – and perhaps in general — power holes occur at frequencies corresponding to the intersection of the fast beam mode with the circuit mode, i.e., at frequencies that are significantly larger than

[5]To test this hypothesis, a series of runs was made in which the ac space charge fields were artificially reduced in strength, by introducing an artificial "fudge factor" multiplying the source terms for the backward wave electric and magnetic fields, as shown in the right hand sides of (27a,b) in [13]. This factor has the effect of artificially reducing the effective plasma frequency of the beam, and so reducing the frequency spacing of the fast and slow beam modes. As the factor is reduced, the spacing of the maximum in the lower band, and minimum in the upper band, is also reduced, strongly suggesting that the identifications of the interactions as fast and slow wave interactions is correct.

[6]We see the same effect using the one-dimensional large signal code CHRISTINE.

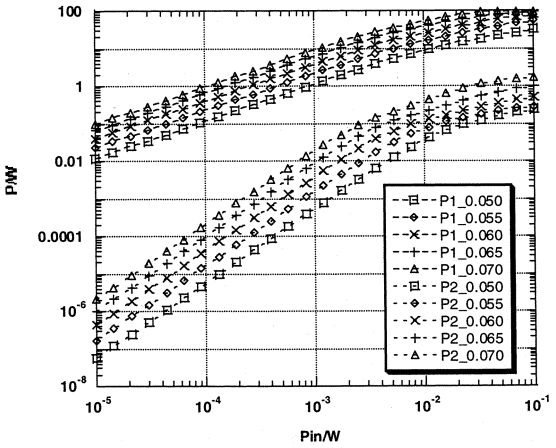

Fig. 3. Output power in fundamental (P1) and second harmonic (P2) as a function of drive power, for different beam radii. The radii in cm are indicated in the legend, e.g., 0.050 cm. Drive frequency = 8.850 GHz; no reflected signals.

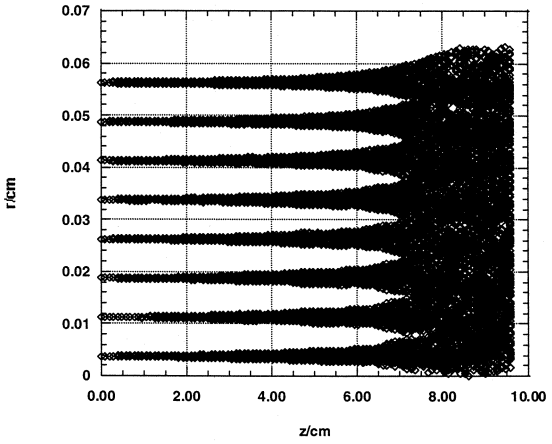

Fig. 4. Beam trajectories in the presence of a large drive signal; Pdrive = 30 mW at 8.862 GHz; no reflected signals.

the frequencies near the intersection of the slow beam mode with the circuit mode for which small signal backward wave gain is found under conditions of zero drive.

III. Simulations of BWO Power Holes in a Helix TWT Using CHRISTINE 3D

The large signal helix TWT code, CHRISTINE 3D, can be used to study the combined effects of harmonic generation, reflections, and backward wave gain that produce a power hole. In the simulations to be presented here, only two signals are present, a fundamental and its second harmonic, both of which have components traveling forward and backward. Power is injected only at the fundamental.

It is of interest to know how much fundamental and second harmonic power is generated as a function of drive power. This is shown in Fig. 3, for a drive frequency of 8.85 GHz, for various initial beam radii. No reflections are included in these simulations. We see that saturation occurs for a drive power of about 100 mW (20 dBm) for the larger beam radii used; for the smaller beam radii, saturation occurs at somewhat higher drive powers. In the following simulations, we have used a drive power of 30 mW (14.8 dBm), for all large signal cases. This appears to be sufficiently large to generate significant amounts of second harmonic power at the output. The simulations below use an initial beam radius of 0.060 cm, but the beam is allowed to expand self-consistently under the influence of the radio frequency (RF) and dc fields, as shown in Fig. 4. The CHRISTINE 3D code includes the (modified Bessel function) variations of the beam-wave interaction strengths with radius, for both forward and backward waves.

It is well known that the BWO gain is sensitive to beam radius, since the strength of the axial RF electric field (E_z) of the backward wave is proportional to radius. It is a simple matter, using CHRISTINE 3D, to compute the small signal backward wave gain as a function of frequency, for different beam radii. Results are shown in Fig. 5. No reflected waves were included

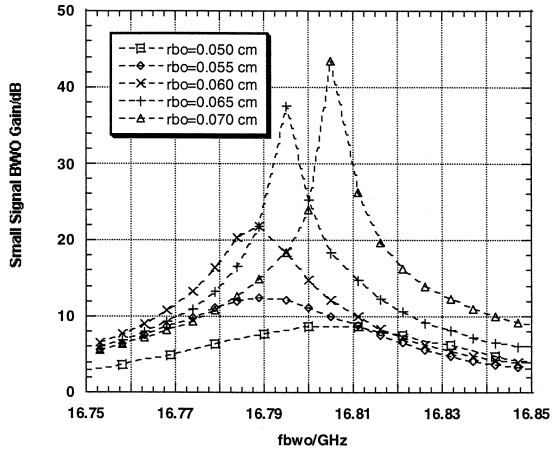

Fig. 5. Small signal backward wave gain versus frequency for various values of beam radius; no drive signal present.

in these simulations, and no drive signal was applied; beam expansion, therefore, was minimal. These results therefore correspond to the classic analysis of Johnson [4]. We see that for beam radius of about 0.065 cm or larger, the gain versus frequency curves develop cusps, suggesting infinite gain, or spontaneous oscillation. For smaller beam radii, the cusps disappear, indicating finite gain across the band. The frequency at which the peak gain occurs is seen to increase slightly with increasing beam radius, when the peak gain is large. Since the results presented in Fig. 5 were obtained under small signal conditions, the frequency band in which BWO gain is obtained corresponds to the lower BWO gain band in Fig. 1.

We now consider what happens when reflections are present, along with harmonic generation and backward wave gain, that is, under conditions that should produce a power hole. In order to simplify the study, and to isolate important effects, the only nonnegligible circuit wave reflection coefficient is taken to be that of the second harmonic signal at the output. For the first series of runs reported below, this reflection coefficient is 0.20, corresponding to a return loss of -14 dB. The reflection coefficients

of the fundamental signal at the output, and of both the fundamental and second harmonic signals at the input are chosen to be very small, corresponding to a return loss of −80 dB for each.

Since the CHRISTINE 3D code solves for the steady state operation of the TWT, it integrates all equations in z, not in time. Consequently, initial conditions for all particles and wave amplitudes must be specified at $z = 0$ in order to start the integration. The initial conditions on the particles' phases are chosen so that the particles uniformly fill a wave period. The injected beam, in the simulations described below, is taken to be azimuthally uniform and of constant density from its center out to its edge; this distribution is free to evolve, of course, as the beam propagates along the interaction space. Other choices for beam initialization are available as options in the code.

The assignment of initial conditions of the wave amplitudes at $z = 0$ can be more complicated. In the case in which only forward waves are present (no reflections), the initial conditions on the wave amplitudes are simply specified by the drive power and phase. When reflections from a circuit discontinuity are present, from a sever or an input or output coupler, for example, the correct initial conditions for the forward and backward wave amplitudes at $z = 0$ are not known at the outset of the computation and must be solved for. This is done in CHRISTINE 3D by using a multi-dimensional Newtons method by which the (complex) values of the initial amplitudes are adjusted iteratively until the boundary conditions at the output are satisfied to some acceptable, user-specified tolerance. A first guess for all amplitudes must be provided by the user. The convergence rate of the algorithm depends on how close the tube is to oscillation. Our experience has been that, well below BWO threshold, the algorithm converges rapidly—within 3–5 iterations. At or above oscillation threshold, however, the algorithm may converge very slowly, or may fail to converge, or its convergence may depend sensitively on the user-provided initial guess for the wave amplitudes. Under large signal conditions, a beam launched with a radius below that required to produce spontaneous oscillation may expand to the threshold of spontaneous oscillation, again complicating convergence of the algorithm.

Using the same set of beam radii used to produce Fig. 5, we have made a series of CHRISTINE 3D runs in which the tube was driven at the fundamental drive frequency, which was varied between 8.8 and 8.9 GHz, at a power of 30 mW (14.8 dBm), which is well into the large signal regime. Results for the output power in the fundamental as a function of the drive frequency are shown in Fig. 6. Power holes can be clearly seen, for (initial) beam radii of 0.060 cm and larger. For beam radii of 0.065 and 0.070 cm, the iterative algorithm used to solve for the wave amplitudes at the input end ($z = 0$) sometimes did not converge, as might be expected for these linearly BWO unstable cases. Non-convergent points are omitted from the plots in Fig. 6. For a beam radius of 0.060 cm, however, for which the small signal BWO gain is finite as shown in Fig. 4, a smooth, finite power hole is seen in Fig. 6. The second harmonic of frequencies in the band of the power hole corresponds the same band in which we found backward wave gain under large signal conditions in Fig. 2, that is, to the *upper* BWO gain band of Fig. 1; no power

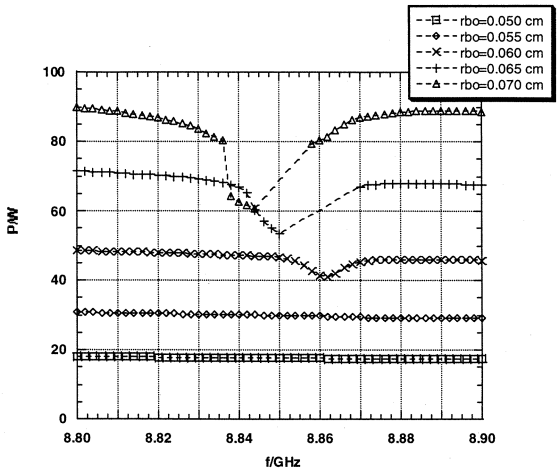

Fig. 6. Output power in fundamental versus frequency, for the same beam radii used in Fig. 2. The reflection coefficient at the output for the second harmonic was 0.20, corresponding to a return loss of 14 dB. For the two largest beam radii used, 0.065 and 0.070 cm, the root finding algorithm used in CHRISTINE 3D did not converge for certain values of drive frequency; these points are omitted in the plot.

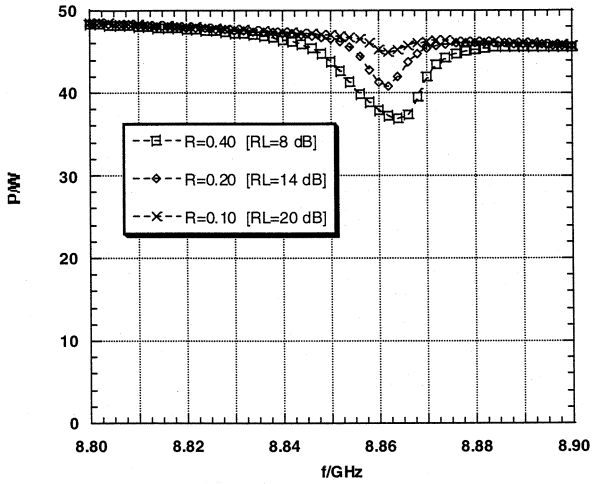

Fig. 7. Output power versus frequency for different values of second harmonic output match. Initial beam radius is 0.060 cm. The curves are labeled by both the voltage reflection coefficient R, and the corresponding return loss, $-20\log(\mathrm{R})$.

holes are observed at lower frequencies. No numerical convergence problems were encountered in this case. The depth of the power hole is about 0.5 dB[7]. We believe that this is the first reported self-consistent, 3-D computer simulation of this phenomenon.

IV. Suppression of Power Holes

Based on our understanding of the physical mechanisms that contribute to the formation of power holes, we can identify possible methods to suppress them. One obvious method is to improve the output match at the second harmonic. Fig. 7 illustrates

[7]An anonymous referee pointed out that the forward wave loses about 5 W, but the power in the backward wave is less than 0.3 W, from which a conclusion may be drawn that the power lost from the forward wave stays largely in the beam, rather than being entirely transferred to the backward wave. This implies that the "lost" forward wave power will be dissipated in the collector, rather than in the circuit/attenuator.

what happens to the power hole, for a beam radius of 0.060 cm, for different values of the output match for the second harmonic, namely 20, 14, and 8 dB. The power hole becomes more shallow as the match is improved, as we would expect. As a practical matter, however, improving the output match at such high frequencies is often very difficult or expensive to do and we are forced to consider other remedies. The most obvious of these is to reduce the backward wave gain.

Many techniques have been successfully used to reduce backward wave gain. Perhaps the most common is the introduction of attenuation or a sever in the circuit. Other techniques include tapering the circuit properties and tapering the magnetic field. The use of a change in magnetic field is attractive since it can affect the interaction of the backward wave with the beam while leaving the forward wave signal growth nominally unaffected [16], unlike the other methods. We have already shown that the backward wave gain depends sensitively on beam radius, so one approach to suppressing the power holes would be to redesign the beam focusing optics to reduce the beam radius. This approach may be complicated, as we have already seen, by the fact that the beam radius generally expands under large signal conditions and this expansion affects the backward wave gain, and the frequency range in which it occurs. There are also of course practical limits to the strength of the magnetic field.

Since it is a relatively unfamiliar idea, and illustrates a 3-D effect using CHRISTINE 3D, we demonstrate the effect of a tapered magnetic field on the power hole. Fig. 8 shows what happens to the power hole for different values of uniform magnetic field. These runs used an initial beam radius of 0.060 cm; the case for a magnetic field of -1400 G is the same case as the corresponding curve in Fig. 6. The location of the hole is seen to shift to lower frequencies as the magnetic field is increased. This shift is attributable to a shift in the backward wave gain band due to the Doppler shift caused by beam rotation.[8] Specifically, Belyavskiy, *et al.* [11] have shown that if the longitudinal magnetic field B is such that the cyclotron frequency is small compared to the BWO frequency, then the whole effect of the magnetic field may be accounted for by a modification of the Pierce b parameter, according to

$$b \to b + l\sigma \tag{2}$$

where

$$\sigma \equiv \eta B/(2\omega C) \tag{3}$$

l is the azimuthal mode number ($+1$ or -1, depending on the sign of B), η is the electron charge to mass ratio, ω is the BWO frequency, and C is the Pierce C parameter. Changing the magnetic field changes the rotation rate, which comes at the expense of the longitudinal velocity. As far as small signal theory goes, then, changing B changes b just as effectively as changing the phase velocity of the circuit wave.

[8]The direction of the rotation matters. In the examples presented in this paper the magnetic field points in the negative z-direction, which produces a clockwise beam rotation when viewed by an observer looking in the negative z-direction. If the field, and consequently the sense of rotation, is reversed, the backward wave gain band shifts to lower frequencies and the peak backward wave gain decreases significantly. This reduction in gain is at least in part due to the decreased values of the backward wave interaction impedance at the lower frequencies. This result suggests that the simple strategy, for solenoid focused tubes, of reversing the direction of the current in the solenoid might, depending on other parameters, greatly reduce (or increase!) backward wave gain.

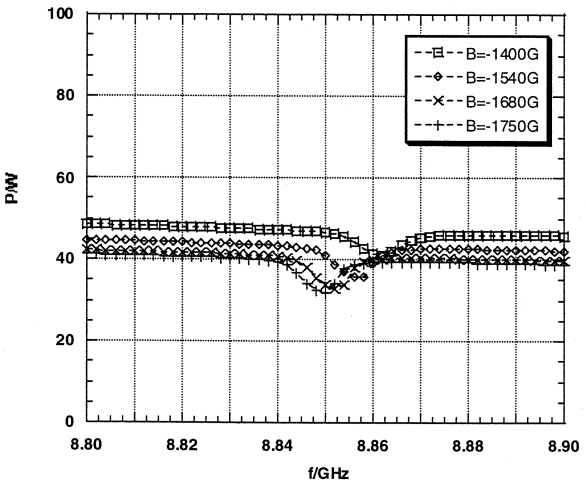

Fig. 8. Output power versus drive frequency, for different values of constant longitudinal magnetic field. Beam was initialized in a rigid rotor configuration with a radius of 0.060 cm.

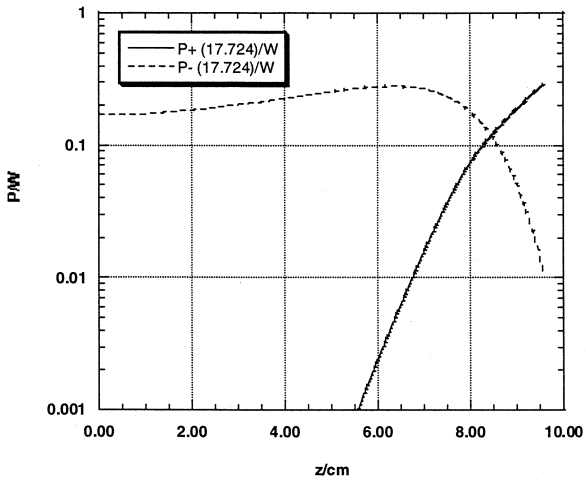

Fig. 9. Forward and backward second harmonic signal powers versus axial location. Drive frequency $= 8.862$ GHz, corresponding to approximately the bottom of the power hole in Fig. 8, B $= -1400$ G.

In the case of Fig. 8, a 20–25% change in magnetic field is observed to shift the location of the power hole by an amount approximately equal to the full width of the hole. This suggests that a field taper of about this amount might reduce the depth of the hole. The question remains, how and where should the field be tapered?

It is a reasonable assumption that, to be most effective, the magnetic field gradient should be largest where the BWO gain is large in the absence of a taper. Fig. 9 illustrates the growth of the forward (solid) and backward (dashed) powers in the untapered case. Most of the backward wave gain is seen to occur in the last 2 cm or so of the interaction space. Based on this observation, the magnetic field profile shown in Fig. 10 was created. The resulting output power versus frequency curve for this magnetic field is shown in Fig. 11. The power hole has been nearly eliminated. The observed reduction of the depth of the power hole is actually due to two simultaneous effects. One is

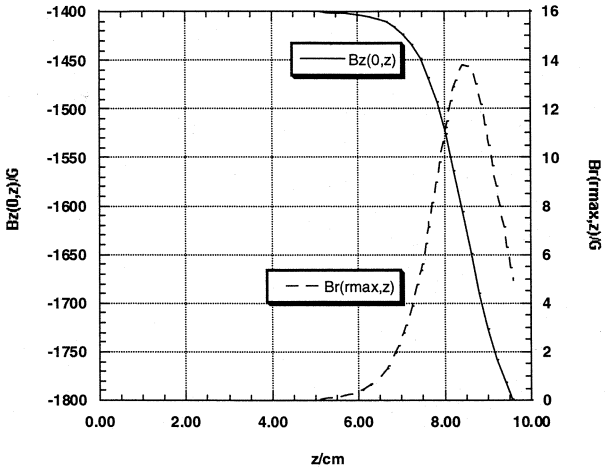

Fig. 10. B-field profile used in the CHRISTINE 3D runs that produced the data for Fig. 11. Both the axial magnetic field, and the corresponding radial magnetic field at the helix radius are shown. The paraxial approximation is used.

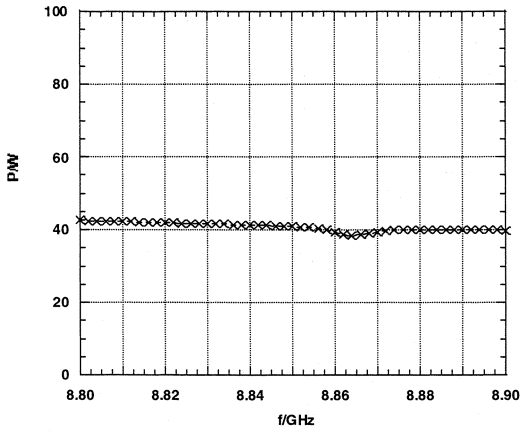

Fig. 11. Output power versus drive frequency, using the magnetic field of Fig. 10.

the change of the backward wave gain due to the changing magnetic field itself, as illustrated in Fig. 8; the other is the reduction in gain due to the compression of the beam produced by the increasing magnetic field. This compression effect competes with the expansion of the beam due to the large RF signal present. The beam profile shown in Fig. 12 illustrates this compression effect. Beam expansion is reversed by the increasing magnetic field (Fig. 12) compared to the uniform field case (Fig. 4).

V. Summary and Conclusions

The physical mechanisms responsible for the phenomenon of power holes in forward wave linear beam amplifiers have been described. Mathematical models of these mechanisms have been implemented in the large signal helix TWT simulation code CHRISTINE 3D. The code has been used successfully to simulate power holes in a helix TWT, including the self-consistent effect of beam expansion. The frequency at which the power hole occurs is seen in an example to be higher than the frequency at which the small signal backward wave gain is maximum. This is due to the de-stabilization of the fast

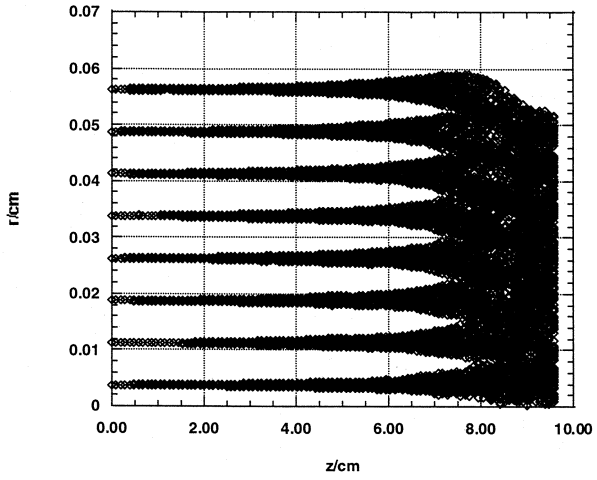

Fig. 12. Beam trajectories in the presence of the magnetic field of Fig. 10.

beam mode by the large amplitude drive signal; an analysis of this phenomenon is in progress and will be reported in a future publication. We have argued that power holes may be suppressed by either improving the broadband output match or by reducing the backward wave gain. Examples of both methods have been illustrated using the CHRISTINE 3D code.

Acknowledgment

The authors acknowledge helpful discussions with C. Armstrong, T. Hargreaves, and P. Walchli, of L3-Com Electron Devices, D. Whaley of Northrop Grumman Corp., N. Dionne of Raytheon Company, and YY Lau of the University of Michigan. We wish to thank two anonymous referees for pointing out that our original interpretation of the frequency shift of the power hole could not be due only to beam expansion, as we conjectured in the original draft of this paper.

References

[1] A. S. Gilmour Jr., *Microwave Tubes*. Norwood, MA: Artech House, 1986.
[2] B. N. Basu, *Electromagnetic Theory and Applications in Beam-Wave Electronics*, Singapore: World Scientific, 1999.
[3] G. S. Nusinovich *et al.*, "Excitation of backward waves in forward wave amplifiers," *Phys. Rev. B*, vol. E58, pp. 6594–6605, 1998.
[4] H. R. Johnson, "Backward-wave oscillators," *Proc. IRE*, pp. 684–697, 1955.
[5] R. W. Grow and D. R. Gunderson, "Starting conditions for backward wave oscillators with large loss and large space charge," *IEEE Trans. Electron Devices*, vol. ED-17, pp. 1032–1039, 1970.
[6] J. A. Swegle, "Starting conditions for relativistic backward-wave oscillators at low current," *Phys. Fluids*, vol. 30, pp. 1201–1211, 1987.
[7] B. Levush, T. M. Antonsen, Jr., A. Bromborsky, W.-R. Lou, and Y. Carmel, "Theory of relativistic backward-wave oscillators with end reflections," *IEEE Trans. Plasma Sci.*, vol. 20, pp. 263–280, June, 1992.
[8] A. S. Gilmour Jr., *Principles of traveling-wave Tubes*. Norwood, MA: Artech House, 1994, ch. 12.
[9] G. Haddad and R. M. Bevensee, "Start-oscillation conditions of tapered backward-wave oscillations," *IEEE Trans. Electron Devices*, vol. ED-9, pp. 389–393, 1963.
[10] G. Haddad and J. E. Rowe, "Start-oscillation conditions in nonuniform backward-wave oscillators," *IEEE Trans. Electron Devices*, vol. ED-11, p. 31, 1964.

[11] E. D. Belyavskiy, I. A. Goncharov, A. E. Martynyuk, V. A. Svirid, and S. N. Khotiaintsev, "Two-dimensional small-signal analysis of backward-wave oscillation in a helix traveling-wave tube under Brillouin-flow, periodic permanent magnetic focusing," *IEEE Trans. Electron Devices*, vol. 48, pp. 1727–1736, Aug. 2001.

[12] N. J. Dionne, R. Harper, and H.-J. Krahn, "Sectored-beam multi-signal TWT analysis," in *IEDM Tech. Dig.*, 1988, pp. 362–365.

[13] D. Chernin, T. M. Antonsen, Jr., B. Levush, and D. R. Whaley, "A three-dimensional multifrequency large signal model for helix traveling-wave tubes," *IEEE Trans. Electron Devices*, vol. 48, pp. 3–11, Jan. 2001.

[14] T. M. Antonsen, Jr., P. Safier, D. Chernin, and B. Levush, "Stability of traveling-wave amplifiers with reflections," *IEEE Trans. Plasma Sci.*, vol. 30, pp. 1089–1107, June 2002.

[15] D. Chernin, T. M. Antonsen, Jr., and B. Levush, "Exact treatment of the dispersion and beam interaction impedance of a thin tape helix surrounded by a radially stratified dielectric," *IEEE Trans. Electron Devices*, vol. 46, pp. 1472–1483, July 1999.

[16] E. D. Belyavskiy and Y. N. Strokoskiy, "Backward-wave self-excitation of the magnetically focused helix traveling-wave tube" (in In translation), *Microwave Electronics (USSR)*, no. 3, pp. 60–65, 1974.

David Chernin received the A.B. and Ph.D. degrees in applied mathematics from Harvard University, Harvard, MA, in 1971 and 1976, respectively.

From 1976 to 1978, he was a Member of the Institute for Advanced Study, Princeton, NJ, where he worked on problems in magnetic confinement fusion. Since 1984 he has been at Science Applications International Corporation, McLean, VA, where he has contributed to multiple research efforts in the theory and simulation of beam-wave interactions in particle accelerators and microwave tubes. He presently serves as the Division Manager of the Center for Electromagnetic Science and Engineering at SAIC.

Dr. Chernin is a member of the American Physical Society and the Society for Industrial and Applied Mathematics.

Thomas M. Antonsen, Jr. (M'87) was born in Hackensack, NJ in 1950. He received the B.S., M.S., and Ph.D. degrees in electrical engineering from Cornell University, Ithaca, NY, in 1973, 1976, and 1977, respectively.

He was a National Research Council Post Doctoral Fellow at the Naval Research Laboratory in 1976–1977, and a Research Scientist in the Research Laboratory of Electronics at the Massachusetts Institute of Technology, Cambridge, from 1977 to 1980. In 1980 he moved to the University of Maryland, College Park, where he joined the faculty of the departments of Electrical Engineering and Physics in 1984. He is currently Professor of physics and electrical and computer engineering. His research interests include the theory of magnetically confined plasmas, the theory and design of high power sources of coherent radiation, nonlinear dynamics in fluids, and the theory of the interaction of intense laser pulses and plasmas. He is the author and coauthor of over 200 journal articles and co-author of the book, *Principles of Free-electron Lasers*. He has held visiting appointments at the Institute for Theoretical Physics (U.C.S.B.), the Ecole Polytechnique Federale de Lausanne, Switzerland, and the Institute de Physique Theorique, Ecole Polytechnique, Palaiseau, France. He has served on the editorial board of *Physical Review Letters*, *Physics of Fluids*, and *Comments on Plasma Physics*.

Dr. Antonsen was selected as a Fellow of the Division of Plasma Physics of the American Physical Society in 1986. In 1999 he was a co-recipient of the Robert L. Woods Award for Excellence in Vacuum Electronics Technology, and in 2003 he was received the IEEE Plasma Science and Applications Award.

Baruch Levush (F'01) received the M.Sc. degree in physics from the Latvian State University, Riga, Latvia, in 1972, and the Ph.D. degree in physics from Tel-Aviv University, Israel, in 1981.

In 1985, he joined the Institute for Plasma Research at the University of Maryland, College Park, where his research focused on the physics of coherent radiation sources and the design of high-power microwave sources, including gyrotrons, traveling-wave tubes, backward wave oscillators and free electron lasers. In 1995, he joined Naval Research Laboratory, Washington, DC, as the Head of the Theory and Design Section of the Vacuum Electronics Branch, Electronics and Technology Division. He now serves as Head of the NRL Vacuum Electronics Branch, where he remains actively involved in developing theoretical models and computational tools for analyzing the operation of vacuum electron devices and in inventing new concepts for high power, high frequency coherent radiation sources. He is responsible for developing a suite of new design codes for vacuum electron devices under the auspices of the Office of Naval Research Modeling and Simulation project. He is the co-author of over 130 journal articles.

Dr. Levush was the recipient of the 1999 Robert L. Woods Award for his role in the successful development of a 10 kW average power, W-band gyro-klystron.